

## Electronic State of the Molecular Oxygen Released by Catalase<sup>†</sup>

Mercedes Alfonso-Prieto,<sup>‡,§</sup> Pietro Vidossich,<sup>‡,§</sup> Antonio Rodríguez-Forteza,<sup>||</sup> Xavi Carpena,<sup>⊥</sup> Ignacio Fita,<sup>⊥</sup> Peter C. Loewen,<sup>#</sup> and Carme Rovira<sup>\*,‡,§,∇</sup>

Laboratori de Simulació Computacional i Modelització (CoSMoLab), Parc Científic de Barcelona, Baldri Reixac 10-12, 08028 Barcelona, Spain, Institut de Química Teòrica i Computacional de la Universitat de Barcelona (IQTCUB), Departament de Química Física i Inorgànica, Universitat Rovira i Virgili, Marcel·lí Domingo s/n, 43007 Tarragona, Spain, Institut de Biologia Molecular (IBMB-CSIC), Institut de Recerca Biomèdica (IRB), Parc Científic de Barcelona, Josep Samitier 1-5, 08028 Barcelona, Spain, Department of Microbiology, University of Manitoba, Winnipeg, MB R3T 2N2, Canada, and Institució Catalana de Recerca i Estudis Avançats (ICREA), Passeig Lluís Companys, 23, 08018 Barcelona, Spain

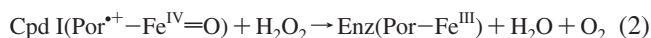
Received: February 20, 2008; Revised Manuscript Received: July 17, 2008

In catalases, the high redox intermediate known as compound I (Cpd I) is reduced back to the resting state by means of hydrogen peroxide in a 2-electron reaction [Cpd I (Por<sup>•+</sup>–Fe<sup>IV</sup>=O) + H<sub>2</sub>O<sub>2</sub> → Enz (Por–Fe<sup>III</sup>) + H<sub>2</sub>O + O<sub>2</sub>]. It has been proposed that this reaction takes place via proton transfer toward the distal His and hydride transfer toward the oxoferryl oxygen (H<sup>+</sup>/H<sup>–</sup> scheme) and some authors have related it to singlet oxygen generation. Here, we consider the possible reaction schemes and qualitatively analyze the electronic state of the species involved to show that the commonly used association of the H<sup>+</sup>/H<sup>–</sup> scheme with singlet oxygen production is not justified. The analysis is complemented with density functional theory (DFT) calculations for a gas-phase active site model of the reactants and products.

### 1. Introduction

Heme containing catalases are present in almost all aerobically respiring organisms.<sup>1</sup> They play critical roles in protecting the cell against the toxic effects of hydrogen peroxide (H<sub>2</sub>O<sub>2</sub>) by degrading it to water and oxygen (2H<sub>2</sub>O<sub>2</sub> → 2H<sub>2</sub>O + O<sub>2</sub>).

The catalatic reaction occurs in two steps. The first step, common to peroxidases, is the formation of compound I (Cpd I), often an oxoferryl porphyrin cation radical, by two electron oxidation of the resting enzyme (reaction 1). It is generally accepted that the distal His (His61, using the residue numbering of *Micrococcus lysodeikticus* catalase;<sup>2</sup> see Figure 1) acts as a general acid–base catalyst in Cpd I formation.<sup>3,4</sup> The second step is the reduction of Cpd I back to the resting state of the enzyme, generating O<sub>2</sub> and a water molecule (reaction 2). Catalases and catalase-peroxidases catalyze this reaction efficiently, whereas other heme proteins such as chloroperoxidase (CPO) and myoglobin (Mb) exhibit low reaction yields.<sup>1,5</sup>



As shown in reaction 2, H<sub>2</sub>O<sub>2</sub> serves as a two-electron reductant in the catalatic reaction. Formally, one electron reduces the porphyrin radical (Figure 2), and the other one contributes

to the change of oxidation state of the iron atom (from Fe<sup>IV</sup> to Fe<sup>III</sup>). The transfer of two electrons from H<sub>2</sub>O<sub>2</sub> is associated with the transfer of two protons, forming O<sub>2</sub>. Nevertheless, it is not known whether H<sub>2</sub>O<sub>2</sub> loses the two electrons as H<sup>+</sup>/H<sup>–</sup> (transfer of a proton and a hydride ion), H<sup>+</sup>/H<sup>•</sup> (double transfer of one hydrogen atom) or other mechanisms. It has been proposed by Fita and Rossmann,<sup>3</sup> and recently supported by Watanabe et al.,<sup>6</sup> that the distal His is also involved in the second step of the catalatic reaction. Because of this, an H<sup>+</sup>/H<sup>–</sup> scheme is assumed, in which H<sup>–</sup> is transferred directly to the oxoferryl unit and the transfer of H<sup>+</sup> is mediated by the distal His (Figure 2).

Even though the generation of O<sub>2</sub> from H<sub>2</sub>O<sub>2</sub> is basically part of the known Latimer series,<sup>7</sup> the spin state of the oxygen molecule generated in the catalase reaction is not clear in the literature. For some authors, proton transfer from H<sub>2</sub>O<sub>2</sub> followed by hydride transfer should generate singlet oxygen [H<sub>2</sub>O<sub>2</sub> (*S* = 0) → <sup>1</sup>O<sub>2</sub> (*S* = 0) + H<sup>+</sup> + H<sup>–</sup> (*S* = 0)], while simultaneous uptake of two hydrogen atoms from H<sub>2</sub>O<sub>2</sub> generates triplet oxygen [H<sub>2</sub>O<sub>2</sub> (*S* = 0) → <sup>3</sup>O<sub>2</sub> (*S* = 1) + H<sup>•</sup> (*S* = 1/2) + H<sup>•</sup> (*S* = 1/2), *S* = spin quantum number]. In other words, two one-electron-transfer steps lead to triplet oxygen, and a pairwise movement of electrons produces singlet oxygen.<sup>8–11</sup> These arguments have been used, for instance, to rationalize a possible reaction mechanism in catalase-peroxidases.<sup>8</sup> Therefore, it might seem a priori that the mechanism involving proton transfer to the distal His (the H<sup>+</sup>/H<sup>–</sup> mechanism) generates singlet oxygen in catalase. Molecular oxygen in the singlet state is a very powerful oxidant. Its damaging action in a variety of biological processes has been well recognized,<sup>12,13</sup> and it has been shown to inactivate enzymes.<sup>14</sup> Even though several experiments have detected singlet oxygen in catalases,<sup>10,11</sup> as pointed out by Jakopitsch et al.,<sup>8</sup> it would not make biological sense to release large amounts of singlet oxygen out of the heme pocket. Clearly,

<sup>†</sup> Part of the "Sason S. Shaik Festschrift".

\* Corresponding author. E-mail: crovira@pcb.ub.es.

<sup>‡</sup> Laboratori de Simulació Computacional i Modelització (CoSMoLab), Parc Científic de Barcelona.

<sup>§</sup> Universitat de Barcelona.

<sup>||</sup> Universitat Rovira i Virgili.

<sup>⊥</sup> Institut de Biologia Molecular (IBMB-CSIC), Institut de Recerca Biomèdica (IRB), Parc Científic de Barcelona.

<sup>#</sup> University of Manitoba.

<sup>∇</sup> Passeig Lluís Companys.

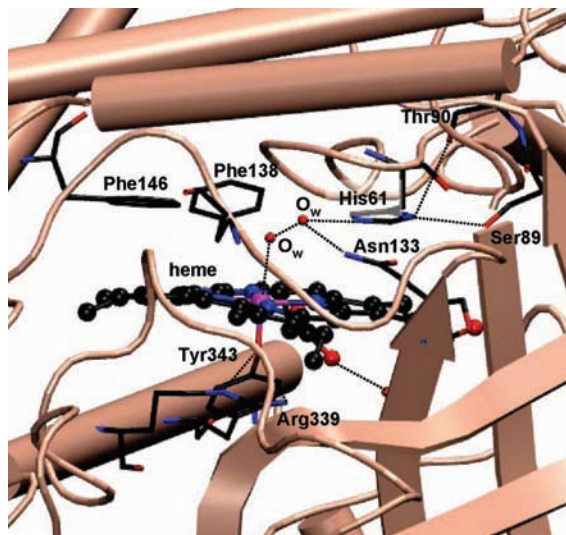


**Figure 1.** Structure around the active site of heme catalases. The residue numbering corresponds to MLC.

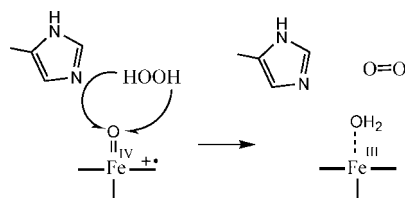


**Figure 2.** Schematic representation of Cpd I reduction by  $\text{H}_2\text{O}_2$  in catalase.

a deeper analysis of the arguments used to predict the spin state of the oxygen molecule is needed.

Here we focus on the problem of the electronic state of the released  $\text{O}_2$  during the reduction of Cpd I in catalases to assess the validity of the arguments that are used to predict the spin state of the released oxygen. We figure out different reaction schemes and qualitatively analyze the spin states of the species involved. It turns out that, even within the spin conservation formalism, when all the species involved in the reaction are taken into account (not only hydrogen peroxide), the produced molecular oxygen may be in the singlet as well as in the triplet state. The analysis is complemented with the calculation of the electronic structures of active site models of the reactants and products by means of density functional theory (DFT). This methodology has been applied in the past to study the reaction intermediates and reactive processes in catalase,<sup>15</sup> peroxidases,<sup>16</sup> catalase-peroxidase<sup>17</sup> and other heme proteins.<sup>18</sup>

## 2. Computational Details

A reduced model of the catalase active site was considered for the calculations. The initial structure was taken from our previous work on catalase Cpd II.<sup>19</sup> Essential residues for the catalase reaction<sup>1,20,21</sup> as well as second shell ligands were included in the model. Specifically, we included the axial Tyr343 residue (replaced by a phenolate anion) and the proximal Arg339 residue (replaced by a methylguanidinium cation) that interacts with the tyrosine oxygen atom (residue numbering corresponding to *Micrococcus lysodeikticus* catalase, MLC). Previous work demonstrated that both residues influence significantly the structure and ligand properties of the heme.<sup>22</sup> The distal side chains of Asn133 and His61 were modeled as ethylamide and methylimidazole, respectively. The Phe138 side chain was also included because it was found to be necessary to keep the  $\text{H}_2\text{O}_2$

substrate in the distal pocket. To better describe the acid/base character of the distal histidine, the residues interacting with its  $\text{N}_\delta\text{-H}$  were also taken into account (Ser89 side chain, replaced by methanol and Thr90 backbone, replaced by formaldehyde). The heme was modeled with an iron porphyrin plus the propionic acid chain that interacts with Ser89 through a bridging water molecule. Additional calculations showed that the protonation state of the propionic heme side chain does not affect the electronic structure of the species analyzed. Hydrogen peroxide was inserted manually in the active site and the structure was optimized by keeping the terminal atoms of the distal and proximal residues fixed to mimic the steric restraints imposed by the protein environment. Structure analysis was performed with VMD.<sup>23</sup>

The calculations were carried out using the Car–Parrinello molecular dynamics method,<sup>24</sup> as implemented in the CPMD code.<sup>25</sup> The Kohn–Sham orbitals were expanded in a plane-wave (PW) basis set with the kinetic-energy cutoff of 70 Ry. The systems were enclosed in an orthorhombic isolated supercell of size  $20.5 \times 19 \times 19 \text{ \AA}^3$  and total charge of +1. The Poisson equation was solved using the Martyna and Tuckerman’s method.<sup>26</sup> We employed ab initio pseudopotentials, generated within the Troullier–Martins scheme,<sup>27</sup> including the nonlinear core correction<sup>28</sup> for the iron atom. Structure optimizations were performed by molecular dynamics with annealing of the atomic velocities, using a time step of 0.072 fs and a value of 800 au for the fictitious electronic mass of the Car–Parrinello Lagrangian. The generalized gradient-corrected approximation of the spin-dependent density functional theory (DFT–LSD), following the formalism of Becke and Perdew,<sup>29</sup> was used. Previous work has demonstrated the reliability of this computational setup in the description of structural, energetic and dynamical properties of heme-based systems.<sup>15a,17,19,22,30</sup> Additional single-point calculations with the B3LYP functional<sup>31,32</sup> and the same PW basis set (not shown here) lead to very similar results with respect to the spin density distributions.

## 3. Results and Discussion

**3.1. Reactants and Products.** The electronic configuration of Cpd I and the possible electronic configurations of the products of the catalase reaction (native enzyme +  $\text{H}_2\text{O}$  +  $\text{O}_2$ ) are depicted in Figure 3. The ground state of catalase Cpd I is known to be a quartet state,<sup>9</sup> with a doublet state very close in energy. Let us assume this situation does not change when  $\text{H}_2\text{O}_2$  enters the distal pocket (Figure 3, left). Let us also assume that the spin state is conserved during the reaction. We will analyze the quartet state surface (an excess of three more unpaired electrons of a given spin, either  $\alpha$  or  $\beta$ ), but analogous results may be obtained working with the doublet state surface (Supporting Information). There are three possible electron configurations of the products that are compatible with a global quartet state. Configuration P1 contains triplet oxygen and doublet heme, both with parallel spins (Figure 3, right). In configuration P2, the oxygen is also in a triplet spin state, but the two unpaired spins are antiparallel with the ones of the heme iron, which is in a high spin state. In configuration P3, all unpaired spins are localized on the heme iron and the oxygen molecule is in a singlet state. An analogous analysis starting with Cpd I in the doublet state (Supporting Information, Figure S1) also gives two configurations with triplet oxygen and one with singlet oxygen. Therefore, a priori the catalytic reaction could generate both types of oxygen spin configurations.

**3.2. Possible Reaction Schemes.** In the reduction of Cpd I in catalases (reaction 2), two hydrogen atoms from  $\text{H}_2\text{O}_2$  are

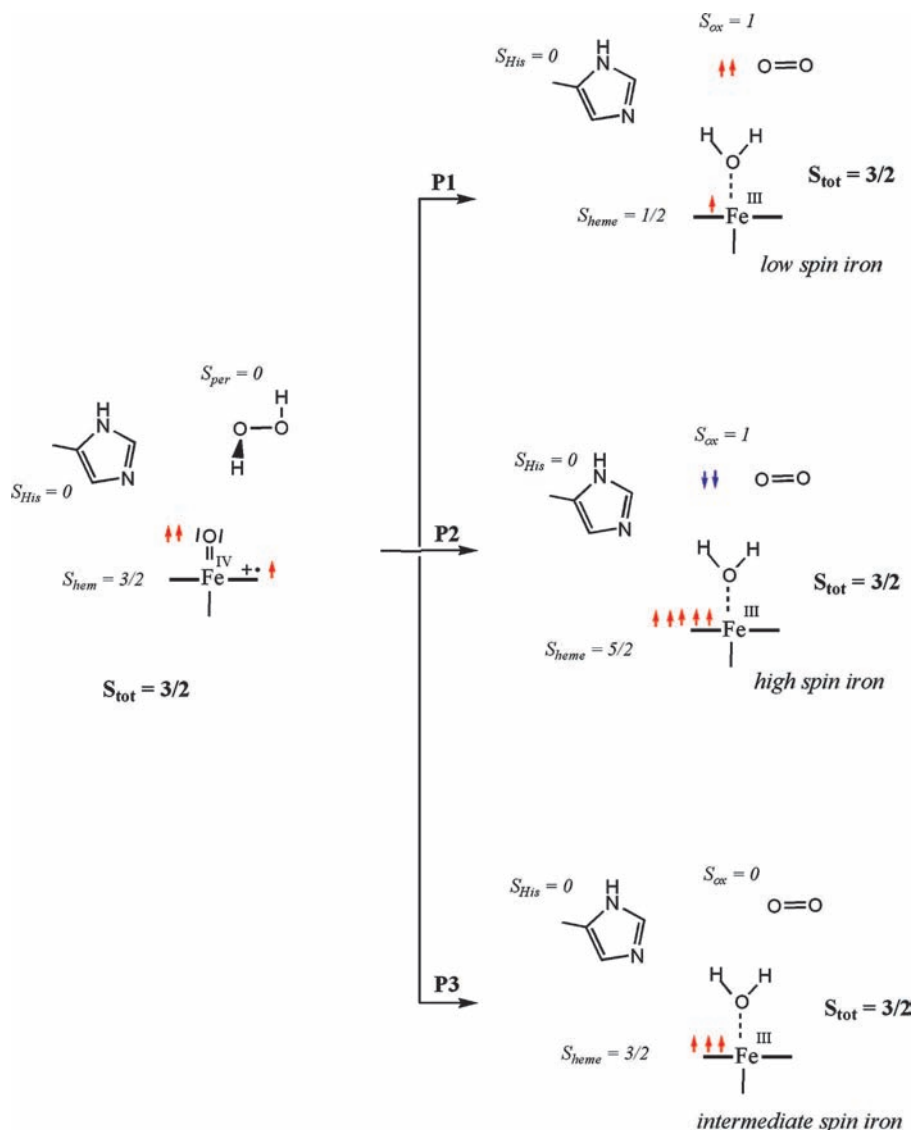


**Figure 3.** Spin reorganization associated to reaction 2 in catalase. R = reactants, P1, P2, P3 = different electronic configuration of the products. The  $\alpha$  spin is represented by red color in the picture.

transferred to the oxoferryl oxygen. Assuming that the distal His is involved in the mechanism, three main reaction schemes (a, b and c) may be envisioned to describe how two protons and two electrons are transferred to the oxoferryl unit.

**(a) Proton Transfer to His and Hydride Transfer to Cpd I ( $H^+/H^-$  Scheme).** Given the  $pK_a$  of His and  $H_2O_2$  in water solution (6.5 and 11.6, respectively), proton transfer from  $H_2O_2$  to His is unfavorable.<sup>33</sup> However, the binding of  $H_2O_2$  to both His and  $Fe=O$  probably decreases its  $pK_a$ . As mentioned in the Introduction, it is believed that the catalytic reaction involves proton transfer to the distal His and hydride transfer to the oxoferryl unit. This scheme would lead to any of the intermediate species shown in Figure 4a (panels a1, a2 and a3 only differ in the distribution of the unpaired spins after  $H^+/H^-$  transfer). To simplify the discussion, we assume that the transfer of both  $H^+$  and  $H^-$  occurs simultaneously. One possibility (a1) is that one of the two transferred electrons couples with the porphyrin unpaired electron and the other goes to an iron-based orbital, decreasing the iron oxidation state. The local spin state of the heme ( $Por-Fe^{III}-OH$ ) is now  $S_{heme} = 1/2$ . To conserve the total spin ( $S_{tot} = 3/2$ ), the product oxygen molecule must be in a triplet state ( $S_{ox} = 1$ ).<sup>34</sup> Alternatively (a2), the electrons could reorganize in a quartet heme ( $S_{heme} = 3/2$ ) and singlet oxygen

( $S_{ox} = 0$ ), or sextet heme and triplet oxygen (a3). In the next reaction step, the proton of  $HisH^+$  would transfer to the hydroxyl group of the heme, releasing a water molecule and leading to the product P1 (P2 and P3 are also possible, considering electronic reorganization at the heme). Therefore, in contrast to the commonly used argument that the  $H^+/H^-$  mechanism generates singlet oxygen, both triplet and singlet oxygen ( $^1O_2$ ,  $^3O_2$ , respectively) can be the product of the catalytic reaction when one takes into account the spin state of all the species in the active center (not only  $H_2O_2$ ).

**(b) Hydrogen Transfer to Both His and Cpd I ( $H^*/H^*$  Mechanism).** Even though  $H^+/H^-$  is considered to be the most likely mechanism, other mechanisms are compatible with the reaction of Figure 2. One of them involves hydrogen transfer to both His and Cpd I ( $H^*/H^*$  mechanism, shown in Figure 4b). As a result, the distal histidine would acquire spin density ( $S_{His} = 1/2$ ). There are five possible intermediates compatible with a global quartet spin state ( $S_{tot} = 3/2$ ). If the electron that transfers to Cpd I couples with the unpaired porphyrin radical (b1 or b3), the result is a local triplet state in the heme (Cpd II-like) and singlet oxygen or triplet oxygen, depending on whether the spin on the distal  $HisH^*$  is parallel or antiparallel to the two unpaired electrons on the hydroxoferryl group, respectively. In

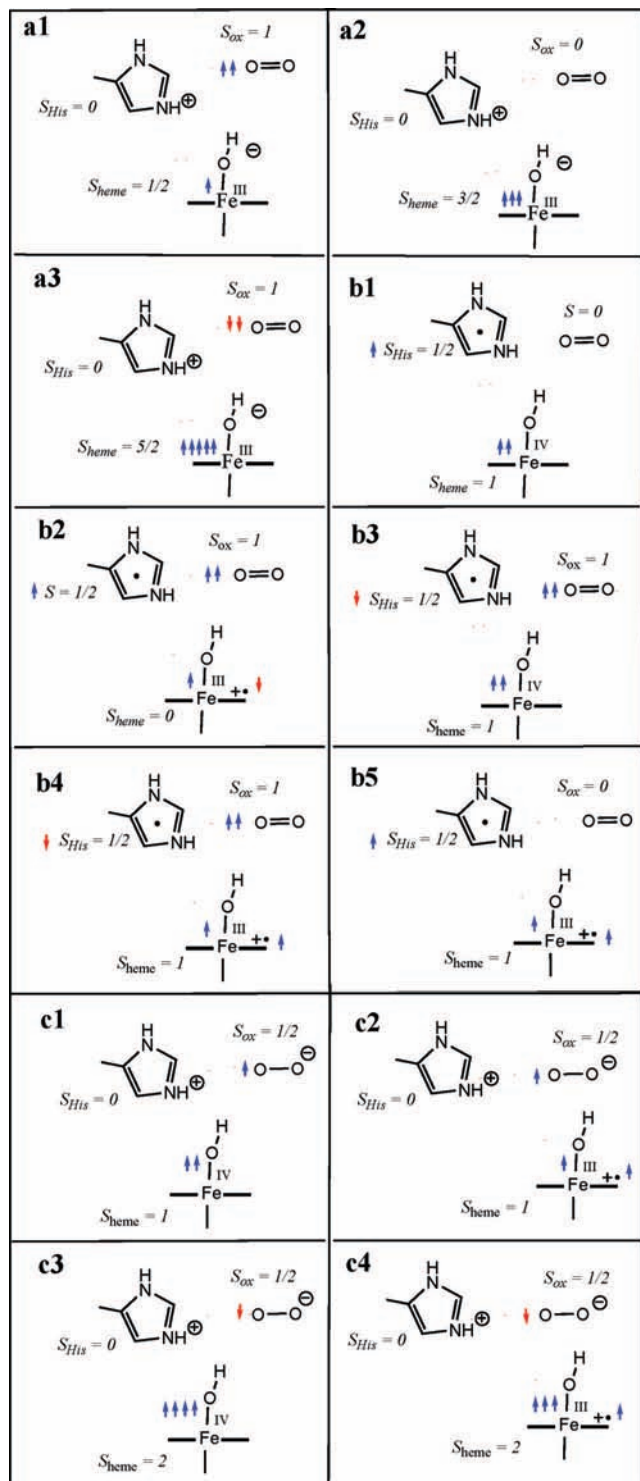


**Figure 4.** Most likely reaction intermediates of reaction 2 in catalase, corresponding to each of the three mechanisms discussed in the text. (a)  $H^+$  transfer to His and  $H^-$  transfer to Cpd I ( $H^+/H^-$ ). (b) Double  $H^+$  transfer ( $H^+/H^+$ ). (c)  $H^+$  transfer to His and  $H^-$  transfer to Cpd I ( $H^+/H^+$ ).

the next step, a hydrogen atom would transfer from His $H^+$  to Cpd II, releasing a water molecule and leading to P3 (from b1) or P1 (from b3). Instead, if the electron that transfers to Cpd I couples with one of the unpaired electrons localized on the oxoferryl unit (b2, b4, b5), the result is a porphyrin radical species in which the porphyrin and oxoferryl unpaired electrons couple antiferromagnetically (b2) or ferromagnetically (b4 and b5). To conserve the total spin, the oxygen molecule could be

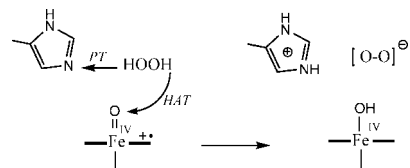


**Figure 5.** Atomic and electron reorganization upon structure optimization of the reactants of reaction 2 (see Introduction): Cpd I ( $Por^{+}-Fe^{IV}=O$ ) +  $H_2O_2$ .

in a triplet state (b2, b3 and b4) or in a singlet state (b1 and b5). Afterward, hydrogen atom transfer from His $H^+$  to the heme would take place, generating the products. Therefore, unlike the common assumption that the  $H^+/H^+$  scheme leads to triplet oxygen, both triplet and singlet oxygen products are compatible with this reaction scheme.

**(c) Hydrogen Transfer to Cpd I and Proton Transfer to His ( $H^+/H^+$  Scheme).** It is also possible that a hydrogen atom is transferred to Cpd I (forming a peroxy radical, HOO $\cdot$ , and Cpd II). The  $pK_a$  of HOO $\cdot$  (4.8) is lower than that of His (6.5); therefore, it is expected that the peroxy radical donates the proton to His, resulting in a superoxide anion molecule ( $O_2^-$ ) (Figure 4c). Two different electronic configurations (c1 and c2) are possible for the intermediate species, depending on which orbital from Cpd I “hosts” the transferred electron. It could be either that this electron couples with the unpaired porphyrin electron (c1 in Figure 4) or that it couples with one of the unpaired electrons of the oxoferryl unit (c2). Considering electronic reorganization at the iron atom, other electronic configurations for the intermediate are possible (c3 and c4). However, they are expected to be higher in energy.<sup>35</sup> Irrespective of this, the intermediate species contains superoxide anion ( $O_2^-$ ). It should be pointed out that the whole  $H^+/H^+$  process is a single electron transfer, whereas reaction 2 (see Introduction) is a two-electron process. It is thus expected that, in the next step, not only the His proton but also a second electron from  $O_2^-$  is transferred to Fe—OH. The reaction could thus possibly proceed via proton-coupled electron transfer, PCET,<sup>36</sup> in which Cpd II receives one proton from His $H^+$  and one electron from  $O_2^-$ , leading to product P3 (Figure 3), in which singlet oxygen is produced, or P1, in which triplet oxygen is produced.

In summary, starting from Cpd I species and  $H_2O_2$  ( $S_{tot} = 3/2$ ), three mechanisms are possible that conserve the total spin. Apart from the two previously proposed mechanisms (a,  $H^+/H^-$ ; b,  $H^+/H^+$ ) there is a third mechanism (c,  $H^+/H^+$ ) in which superoxide anion would be formed. Each of the three mechanisms can lead to either triplet or singlet oxygen as reaction product. Nevertheless, the most important result of this analysis is that the commonly assumed association of the  $H^+/H^-$  scheme with singlet oxygen production is not justified. Similar conclusions are obtained when the reaction takes place in the  $S = 1/2$  surface (see Supporting Information).

**3.3. Calculations of the Reactants and Products.** To illustrate the above considerations, we performed DFT calculations of the reactants and products using the active site model described in section 2. We did not attempt to rank in energy all the possible electronic configurations discussed so far (Figure 4); thus the calculations converge to the most stable electronic configuration of each species for a given total spin. The reactant state (Cpd I/ $H_2O_2$  complex) was modeled by introducing  $H_2O_2$  in the heme distal pocket (as described in section 2) and optimizing the structure. Hydrogen peroxide was found to be not stable in the distal pocket because it loses its two hydrogen atoms, as depicted in Figure 5. The system thus spontaneously initiates the reaction. Analysis of the final structure and spin

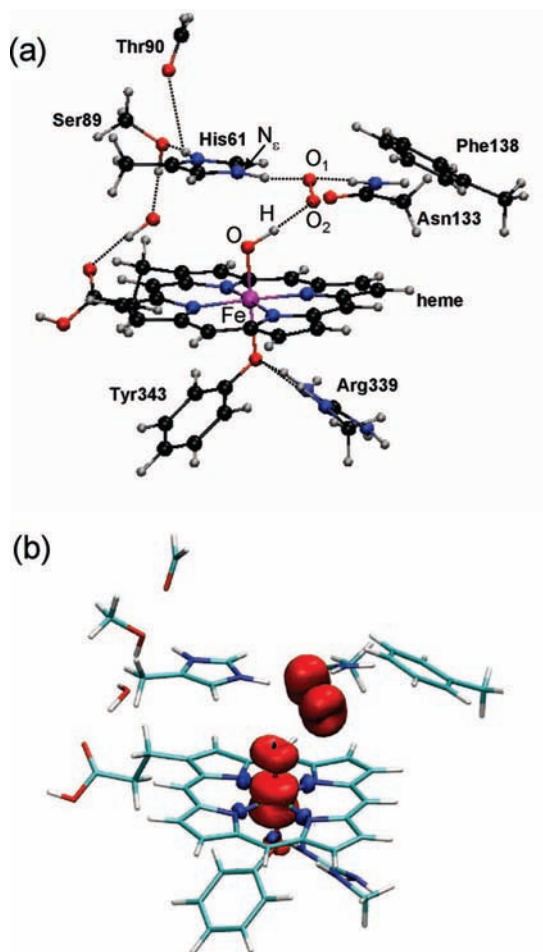


**Figure 6.** Optimized structure (a) and spin density (b) of the intermediate species of Figure 5.

**TABLE 1: Selected Distances (Covalent Bonds and Hydrogen Bonds) Defining the Optimized Structure of the Intermediate Species (Figure 6) and the Products (Figure 7) for  $S_{\text{tot}} = 3/2$**

distance	intermediate	products
Fe–O	1.75	2.05
Fe–O <sub>Tyr</sub>	2.04	1.96
Fe–N <sub>Por</sub>	1.99–2.03	2.00–2.02
Fe out-of-plane	0.06	0.03
O <sub>1</sub> –O <sub>2</sub>	1.30	1.24
N <sub>e</sub> H···O <sub>1</sub>	1.62	
N <sub>e</sub> –H	1.07	
O–H	1.03	0.99
H···O <sub>2</sub>	1.62	1.99
H···N <sub>e</sub>		1.91
O <sub>1</sub> ···H(Asn)	2.01	2.72

density (Figure 6) shows that one proton has been transferred to the distal His, whereas hydrogen atom transfer (HAT) and not hydride transfer to Cpd I takes place. Therefore, our calculations, based on a simplified model, show a first step of the reaction consistent with the third reaction scheme (Figure 4, species c1), in which superoxide anion and a Cpd II-like heme are formed. The optimized structure (Table 1) shows that the Fe–O distance (1.75 Å) is very similar to a hydroxoferryl Cpd II (1.79 Å) and the O–O distance (1.30 Å) is very similar to a superoxide anion (1.32 Å, computed with the same method). The ground state of this species [Cpd II (Por–Fe<sup>IV</sup>–OH) + O<sub>2</sub><sup>−</sup> + HisH<sup>+</sup>] was found to be the quartet ( $S_{\text{tot}} = 3/2$ ), with the doublet state very close in energy (within 2 kcal/mol).

It could be argued that the well-known self-interaction error (SIE) associated to DFT could affect the results obtained (for instance, the hydrogen atom transfer from H<sub>2</sub>O<sub>2</sub> to Cpd I to generate a hydroxoferryl Cpd II<sup>19</sup>). Because the inclusion of a Hartree–Fock (HF) exchange part in the exchange–correlation functional decreases the SIE,<sup>37</sup> we performed additional B3LYP/PW single-point calculations of the reactants, which gave the same electronic distribution (i.e., Cpd II + superoxide). This result does not exclude completely that the SIE could be present in our calculation. Nevertheless, Cpd I of heme-b catalases (such as the one studied here) can be spontaneously reduced to Cpd II by a residue of the protein in the absence of hydrogen peroxide,<sup>38,15a</sup> and Cpd II is expected to be protonated.<sup>15c,d,19</sup> Moreover, catalases also exhibit peroxidatic activity, in which Cpd I is one-electron reduced to Cpd II by an exogenous organic substrate. Therefore, it is not surprising that Cpd II is formed via hydrogen atom transfer from H<sub>2</sub>O<sub>2</sub> to Cpd I.

As mentioned before, the subsequent step to generate the product of the reaction (P1, P2 or P3 in Figure 3) from c1 is expected to be the transfer of the His proton to the hydroxoferryl unit, as well as the transfer of one electron from the superoxide anion to Fe<sup>IV</sup>–OH. It is likely that this occurs via a PCET mechanism, as found in other heme proteins.<sup>39,40</sup> To obtain the reaction products, we moved the histidine proton to the hydroxoferryl oxygen and reoptimized the structure. The final optimized structure is shown in Figure 7 and Table 1 lists the main structural parameters. The newly formed water molecule is coordinated to the iron atom (Fe–OH<sub>2</sub> = 2.05 Å) and the superoxide anion has converted to neutral oxygen (O–O = 1.24 Å) that remains hydrogen bonded to the distal asparagine and the pocket water (Figure 7). The side chain of the distal His moves slightly with respect to its position in the intermediate species c1 (Figure 7) and hydrogen bonds to the pocket water, indicating a putative proton-transfer pathway. It is to be noted that in the X-ray structure of the native enzyme the pocket water is hydrogen bonded to both distal residues (histidine and asparagine) and it is further away from the iron (Fe···O = 3 Å), most likely due to the absence of the oxygen molecule in the distal pocket. Analysis of the spin density distribution (Figure 8b and Table 2) shows that the oxygen molecule is in the triplet state (spin density ≈ 2e) and the iron is locally in a doublet Fe<sup>III</sup> state. Other spin states (doublet,  $S_{\text{tot}} = 1/2$ , and sextet,  $S_{\text{tot}} = 5/2$ ) were found to be very close in energy (all within 3 kcal/mol), with the octuplet state ( $S_{\text{tot}} = 7/2$ ) lying higher in energy (9 kcal/mol above the quartet). Except for the octuplet state, in all cases the local spin state of the iron atom was found to be either low spin or intermediate spin. Even though the spin state

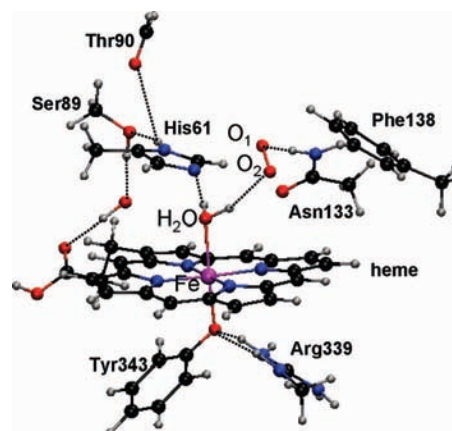


**Figure 7.** Optimized structure of the product of the reaction 2 (see Introduction): Enz(Por–Fe<sup>III</sup>) + H<sub>2</sub>O + O<sub>2</sub>.

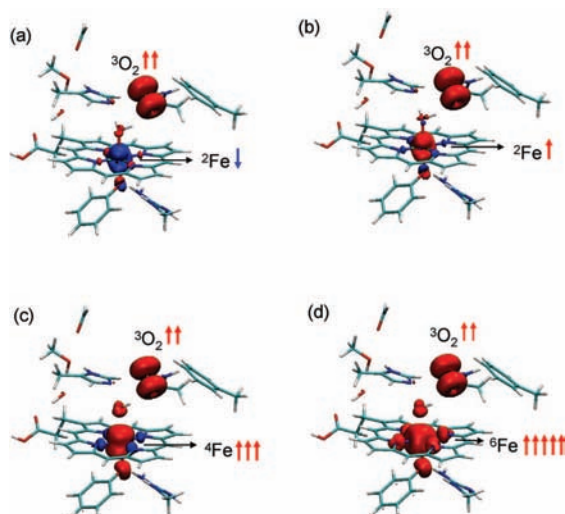


**Figure 8.** Spin density distribution of the product of the reaction for different total spin states: (a) doublet state ( $S_{\text{tot}} = 1/2$ ), (b) quartet state ( $S_{\text{tot}} = 3/2$ ), (c) sextet state ( $S_{\text{tot}} = 5/2$ ), (d) octuplet state ( $S_{\text{tot}} = 7/2$ ).

**TABLE 2: Atomic Spin Densities (Number of Unpaired Electrons in Each Atom or Pair of Atoms) for  $S_{\text{tot}} = 3/2$**

atom	intermediate	products
Fe	1.45	1.06
O	0.26	0.02
FeO	1.71	1.08
O <sub>Tyr</sub>	0.03	0.02
O <sub>1</sub> O <sub>2</sub>	1.28	1.89
N <sub>ε</sub>	0.01	0.01

of the products is not known experimentally, we can assume that it is the same as that of the resting state of the enzyme, i.e., a high spin iron.<sup>41</sup> The fact that this is not well reproduced in the calculations could be due to the well-known drawback of DFT in describing high spin states of the iron atom in porphyrin systems.<sup>30,42</sup> Alternatively, it could be that the spin state changes when O<sub>2</sub> is still in the heme pocket. As mentioned above, in the final optimized structure of the products the water molecule is hydrogen bonded with the oxygen molecule instead of being hydrogen bonded to the distal residues as in the X-ray structure of the native enzyme. As a result, the pocket water maintains the coordination to the iron atom (hexacoordinated Fe<sup>III</sup>) (i.e., simply there is not enough space in the active site for the two molecules). The exit of the oxygen molecule from the active site might allow the water molecule to break the bond with the iron, yielding a pentacoordinated Fe<sup>III</sup>. The change in the coordination number of the iron will modify the splitting of the d-orbitals of the iron, further stabilizing the higher spin states. Indeed, the optimized structures in the sextet states exhibit the longest iron–water distance (2.45 and 2.33 Å).

#### 4. Summary and Conclusions

In catalases, the reduction of the high redox intermediate Cpd I by hydrogen peroxide involves the transfer of two electrons and two protons from the peroxide to the oxoferryl porphyrin cation radical to restore the heme resting state with the release of a water molecule and molecular oxygen. The actual mechanism of the reaction is not known. The electronic state of the oxygen released has been related to the way in which electron and proton transfers are coupled in the reaction. On the basis of an analysis of the nature and the geometry of the active site, the coupling of protons and electrons according to an H<sup>+</sup>/H<sup>-</sup> scheme (transfer of a proton to His and a hydride to the oxoferryl

oxygen) has been assumed as more favorable than an H<sup>+</sup>/H<sup>-</sup> scheme (double transfer of one hydrogen atom) because of the ability of the nearby His as a proton driver.<sup>3</sup> The H<sup>+</sup>/H<sup>-</sup> transfer has been associated with the release of singlet oxygen, which has indeed been detected.<sup>9–11</sup> This poses a biological question, because the generation of large amounts of singlet oxygen would inactivate the enzyme.

In this work we analyzed the electronic configuration of the oxygen released in monofunctional catalases taking into account the spin state of all active species (not only H<sub>2</sub>O<sub>2</sub>). It is shown that, in contrast to what has been often assumed, the H<sup>+</sup>/H<sup>-</sup> scheme does not necessarily generate singlet oxygen. Moreover, a third stepwise scheme involving first proton and hydrogen atom transfer, then proton and electron transfer (possibly in a concerted fashion), is also compatible with the conservation of the total spin. DFT calculations on a reduced active site model predict this to be the route and that triplet oxygen is the product of the reaction, irrespective of the global spin state of the products. Further studies, aimed at the reconstruction of the energetics of the reaction and based on more realistic models, are needed to verify this prediction. Indeed, because of the simplified model (e.g., the absence of protein environment) and the approximations of the method (DFT) used, it could be that the reaction follows a different path. Recently, it has been shown by de Visser<sup>15b</sup> that external perturbations have a significant influence on the electronic properties of catalase Cpd I. Electric fields and dielectric medium may alter the ordering of spin states, with possible consequences on the enzyme activity. Thus, it is important to include in the calculations, possibly through a hybrid QM/MM approach, the solvent and protein environment, to account for long-range electrostatic effects. However, our qualitative analysis, conducted both on the quartet and on the doublet spin states, show that the a priori assumption that the H<sup>+</sup>/H<sup>-</sup> scheme leads to the generation of singlet oxygen in catalases, whereas the H<sup>•</sup>/H<sup>•</sup> schemes leads to triplet oxygen, is not justified.

**Acknowledgment.** This work was supported by Grants 2005SGR-00036 from the *Generalitat de Catalunya (GENCAT)*, FIS2005-00655, BFU2004-06377-C02-02 from the *Ministerio de Educación y Ciencia (MEC)*, Spain, by grant OGP9600 from the Natural Sciences and Engineering Research Council of Canada (to P.C.L.) and by the Canadian Research Chair Program (to P.C.L.). Contracts from the Juan de la Cierva program of MEC (to P.V.), the I3P program of the Spanish Research Council (to X.C.), the Ramón y Cajal program (ref RYC-2005-002572, to A.R.-F.) and the F.I. fellowship program of the GENCAT (to M.A.-P.) are acknowledged. We also acknowledge the computer support, technical expertise, and assistance provided by the Barcelona Supercomputing Center-Centro Nacional de Supercomputación (BSC-CNS).

**Supporting Information Available:** Figure S1 of possible electronic configurations for a doublet total spin ( $S_{\text{tot}} = 1/2$ ). Figure S2 of the three main mechanisms for proton/electron transfer. Optimized structure coordinates for the products in different spin states. This information is available free of charge via the Internet at <http://pubs.acs.org>.

#### References and Notes

- Nichols, P.; Fita, I.; Loewen, P. C. *Enzymology and Structure of Catalases*. In *Advances in Inorganic Chemistry*; Sykes, A. G., Mauk, G., Eds.; Academic Press: New York, 2001; pp 51–106.
- Murshudov, G. N.; Grebenko, A. I.; Branningan, J. A.; Antson, A. A.; Barynin, V. V.; Dodson, G. G.; Dauter, Z.; Wilson, K. S.; Melik-Adamyanyan, W. R. *Acta Crystallogr. D* **2002**, *58*, 1972–1982.

- (3) Fita, I.; Rossmann, M. G. *J. Mol. Biol.* **1985**, *185*, 21–37.
- (4) Jones, P.; Dunford, H. B. *J. Inorg. Biochem.* **2006**, *99*, 2292–2298.
- (5) Hersleth, H. P.; Uchida, T.; Røhr, A. K.; Teschner, T.; Schünemann, V.; Kitagawa, T.; Trautwein, A. X.; Görbitz, C. H.; Andersson, K. K. *J. Biol. Chem.* **2007**, *282*, 23372–23386.
- (6) Kato, S.; Ueno, T.; Fukuzumi, S.; Watanabe, Y. *J. Biol. Chem.* **2004**, *279*, 52376–52381.
- (7) (a) Latimer, W. M. *The Oxidation States of the Elements and their Potentials in Aqueous Solutions*, 1st ed.; Prentice-Hall, New York, 1938. (b) Petlicki, J.; van de Ven, T. G. M. *J. Chem. Soc., Faraday Trans.* **1998**, *94*, 2763.
- (8) Jakopitsch, C.; Auer, M.; Regelsberger, G.; Jantschko, W.; Furtmüller, P. G.; Ruker, F.; Obinger, C. *Biochemistry* **2003**, *42*, 5292–5300.
- (9) Khan, A. U.; Gebauer, P.; Hager, L. P. *Proc. Natl. Acad. Sci. U.S.A.* **1983**, *80*, 5195–5197.
- (10) Michán, S.; Lledías, F.; Baldwin, J. D.; Natviq, D. O.; Hansberg, W. *Free Radical Biol. Med.* **2002**, *33*, 521–532.
- (11) Lledías, F.; Rangel, P.; Hansberg, W. *J. Biol. Chem.* **1998**, *273*, 10630–10637.
- (12) Alia; Mohanty, P.; Matysik, J. *Amino Acids* **2001**, *21*, 195–200.
- (13) Adam, W.; Kazakov, D. V.; Kazakov, V. P. *Chem. Rev.* **2005**, *105*, 3371–3387.
- (14) Jones, P.; Suggett, A. *Biochem. J.* **1968**, *110*, 621–629.
- (15) (a) Alfonso-Prieto, M.; Borovik, A.; Carpena, X.; Murshudov, G.; Melik-Adamyán, W.; Fita, I.; Rovira, C.; Loewen, P. C. *J. Am. Chem. Soc.* **2007**, *129*, 4193–4205. (b) de Visser, S. P. *Inorg. Chem.* **2006**, *45*, 9551–9557. (c) Horner, O.; Oddou, J. L.; Mousesca, J. M.; Jouve, H. M. *J. Inorg. Biochem.* **2006**, *100*, 477–479. (d) Horner, O.; Mousesca, J. M.; Solari, P. L.; Orío, M.; Oddou, J. L.; Bonville, P.; Jouve, H. M. *J. Biol. Inorg. Chem.* **2007**, *12*, 509–525.
- (16) See for instance (a) Derat, E.; Shaik, S.; Rovira, C.; Vidossich, P.; Alfonso-Prieto, M. *J. Am. Chem. Soc.* **2007**, *129*, 6346. (b) Derat, E.; Shaik, S. *J. Am. Chem. Soc.* **2006**, *128*, 13940–13949. (c) Derat, E.; Cohen, S.; Shaik, S.; Altun, A.; Thiel, W. *J. Am. Chem. Soc.* **2005**, *127*, 13611–13621. (d) Bathelt, C. M.; Mulholland, A. J.; Harvey, J. N.; Dalton, T. **2005**, 3470–3476. (e) Behan, R. K.; Green, M. T. *J. Inorg. Biochem.* **2006**, *100*, 448–459.
- (17) Vidossich, P.; Alfonso-Prieto, M.; Carpena, X.; Loewen, P. C.; Fita, I.; Rovira, C. *J. Am. Chem. Soc.* **2007**, *129*, 13436–13446.
- (18) See for instance (a) Cho, K.-B.; Derat, E.; Shaik, S. *J. Am. Chem. Soc.* **2007**, *129*, 3182. (b) Unno, M.; Chen, H.; Kusama, S.; Shaik, S.; Ikeda-Saito, M. *J. Am. Chem. Soc.* **2007**, *129*, 13394–13395. (c) Shaik, S.; Kumar, D.; de Visser, S. P.; Altun, A.; Thiel, W. *Chem. Rev.* **2005**, *105*, 2279–2328.
- (19) Rovira, C. *Chemphyschem* **2005**, *6*, 1820–1826.
- (20) Zámocky, M.; Koller, F. *Prog. Biophys. Mol. Biol.* **1999**, *72*, 19–66.
- (21) Loewen, P. C.; Switala, J.; von Ossowski, I.; Hillar, A.; Christie, A.; Tattrie, B.; Nicholls, P. *Biochemistry* **1993**, *32*, 10159–10164.
- (22) Rovira, C.; Fita, I. *J. Phys. Chem. B* **2003**, *107*, 5300–5305.
- (23) Humphrey, W.; Dalke, A.; Schulten, K. *J. Mol. Graphics* **1996**, *14*, 33–38.
- (24) Car, R.; Parrinello, M. *Phys. Rev. Lett.* **1985**, *55*, 2471–2474.
- (25) CPMD 3.10; MPI für Festkörperforschung Stuttgart and IBM Zurich Research Laboratory, 2006.
- (26) G.J. Martyna; G. J.; Tuckerman, M. E. *J. Chem. Phys.* **1999**, *110*, 2810.
- (27) Troullier, N.; Martins, J. L. *Phys. Rev. B* **1991**, *43*, 1993–2006.
- (28) Louie, S. G.; Froyen, S.; Cohen, M. L. *Phys. Rev. B* **1982**, *26*, 1738–1742.
- (29) (a) Becke, A. D. *J. Chem. Phys.* **1986**, *84*, 4524–4529. (b) Perdew, J. P. *Phys. Rev. B* **1986**, *33*, 8822–8824.
- (30) Rovira, C.; Kunc, K.; Hutter, J.; Ballone, P.; Parrinello, M. *J. Phys. Chem. A* **1997**, *101*, 8914–8925.
- (31) (a) Becke, A. D. *Phys. Rev. A* **1988**, *36*, 3098–3100. (b) Lee, C.; Yang, W.; Parr, R. G. *Phys. Rev. B* **1988**, *37*, 785–789. (c) Becke, A. D. *J. Chem. Phys.* **1993**, *98*, 5648–5652.
- (32) Todorova, T.; Seitsonen, A. P.; Hutter, J.; Kuo, I.-F. W.; Mundy, C. J. *J. Phys. Chem. B* **2006**, *110*, 3685–3691.
- (33) Jones, P.; Dunford, B. *J. Inorg. Biochem.* **2005**, *99*, 2292–2298.
- (34) An alternative situation with five unpaired electrons in the heme (four on the iron–oxygen unit and one in the porphyrin) is excluded because it is expected to be a high energy configuration for the heme.
- (35) Filatov, M.; Harris, N.; Shaik, S. *Angew. Chem., Int. Ed.* **1999**, *38*, 3510–3512.
- (36) (a) Mayer, J. M. *Annu. Rev. Phys. Chem.* **2004**, *55*, 363–390. (b) Reece, S. Y.; Hodgkiss, J. M.; Stubbe, J. A.; Nocera, D. G. *Philos. Trans. R. Soc.* **2006**, *361*, 1351–1364.
- (37) Lundberg, M.; Siegbahn, P. E. M. *J. Chem. Phys.* **2005**, *122*, 224103.
- (38) Ivancich, A.; Jouve, H. M.; Sartor, B.; Gaillard, J. *Biochemistry* **1997**, *36*, 9356–9364.
- (39) Derat, E.; Shaik, S. *J. Am. Chem. Soc.* **2007**, *128*, 13940–13949.
- (40) Cho, K. B.; Derat, E.; Shaik, S. *J. Am. Chem. Soc.* **2007**, *129*, 3182–3188.
- (41) Sharma, K. D.; Andersson, L. A.; Loehr, T. M.; Termer, J.; Goff, H. M. *J. Biol. Chem.* **1989**, *264*, 12772–12779.
- (42) Ghosh, A.; Vangberg, T.; Gonzalez, E.; Taylor, P. *J. Porphyrins Phthalocyanines* **2001**, *5*, 345.